Experimental Study of Laminar Lean Premixed Methylmethacrylate/Oxygen/Argon Flame at Low Pressure

Tianfang Wang, Shufen Li,* Zhenkun Lin, Donglin Han, and Xu Han

Department of Chemical Physics, University of Science and Technology of China, Hefei Anhui 230026, People's Republic of China

Received: October 11, 2007; In Final Form: November 17, 2007

A fuel-lean laminar premixed methylmethacrylate/oxygen/argon flame at 2.67 kPa with an equivalence ratio (ϕ) of 0.75 has been investigated with the tunable synchrotron vacuum ultraviolet (VUV) photoionization and molecular beam sampling mass spectrometry techniques. Isomers of most observed species in the flame have been identified by measurements of photoionization mass spectra and the near-threshold photoionization efficiency spectra. Mole fraction profiles for about 42 flame species are displayed. Free radicals such as CH_3, C_2H_3, C_2H_5, C_3H_3, C_3H_5, C_2H_3O, C_4H_7, C_3H_5O, C_3H_7O, C_4H_3O, C_4H_9O, $C_4H_5O_2$, $C_4H_7O_2$, and $C_5H_7O_2$, which should be of importance in understanding the formation mechanism of some toxic substances, were detected in the flame. Moreover, no isomers of any PAHs have been detected in the lean flame. Combined with the mole fraction profiles, the formation mechanisms of the free radicals, oxygenated compounds, and other molecular intermediates are proposed and will provide important information on modeling the combustion kinetics of methylmethacrylate (MMA).

Introduction

Poly(methylmethacrylate), simplified as PMMA, is an inexpensive polymer and vastly used as building material and consumer products because of its excellent transparency, good weathering resistance, and machinability.[1−3] It has the chemical structure demonstrated as follows:

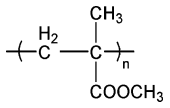

Furthermore, PMMA has a brilliant future in acting as low cost explosives and fuels. In the 1970s, Brokenbrow and colleagues studied the combustion behaviors of some kinds of explosives and propellants containing plastic materials, which included PMMA, and suggested a possible interaction mechanism.[4] In recent years, renewed interest in hybrid rockets has occurred because of their more benign combustion products, reduced cost, and low vulnerability compared with conventional rocket motors,[5] and micropropulsion systems have been developed a lot to fulfill the requirements of maintaining the formate and tracking for spacecrafts.[6−8] These systems are planned to have masses less than 50 kg with attitude control estimated to be in the 1−10 mN thrust class.[9] Due to its low decomposition rate as the temperature increases and the stable combustion rate of MMA, PMMA is considered as a proper material for this application. Surrey Satellites Technology Limited (U.K.) carried out research on GOX-PMMA hybrid motors and put them to use in actual rocket launching.[10] Nakamura et al. employed simulation and experimental studies of the ignition characteristics of a thin PMMA sheet using a CO_2 laser as an external radiant source in microgravity, with the aim of applications in spacecraft, especially the International Space Station.[11] Therefore, the combustion characteristics of PMMA are important to the studies of flame spreading, fire suppression, emission of toxic chemicals in fire hazards, solid propellant combustion, etc. Meanwhile, it will help to optimally design some solid fuel ramjets and hybrid rocket engines.

In explosions, propellants combustion, and fire hazards, the combustion behaviors of materials, which is approximate to rapid heating processes, always include a one-step pyrolysis reaction. Under this condition, many polymers, especially those synthesized by monomer polymerization methods, tend to decompose to monomers first. In PMMA combustion chemistry, once the surface temperature reaches its decomposition (i.e., pyrolysis) temperature when heated by an external ignition source, the gaseous degradation products, most of which is MMA (the monomer of PMMA, with the chemical formula of $C_5H_8O_2$), are evolved from the surface and mix with the ambient oxygen to form the combustible mixture.[12] It has been described by an irreversible, exothermic gas-phase reaction model.[13−15]

MMA is a substance of low boiling point and high saturated vapor pressure. It is confirmed to be the major product, whose the mole fraction should be more than 0.90, in the initial step of PMMA combustion, and then MMA decomposes to generate a lot of small gaseous combustible products.[16] Some studies indicated that the gas phase heat absorption of these products in the fuel−air mixture near the PMMA sheet played an important role in the ignition process, and in some cases, the inclusion of the absorption could be a decisive factor for the success, or failure, of ignition.[17−19] Therefore, for obtaining the combustion mechanism and kinetics of PMMA, it is of great importance to investigate in depth the combustion processes, chemical reactions, and the mole fraction distributions of relevant substances in MMA flame.

As its application area extends, the disadvantages of PMMA become more significant. Whereas PMMA is a kind of thermoplastic material, it can only be put to regular use below vitrification point. The thermal distortion temperature of PMMA

* Corresponding author. E-mail: lsf@ustc.edu.cn. Fax: +86-551-3631760. Tel: +86-551-3601137.

10.1021/jp709927j CCC: $40.75
Published on Web 01/16/2008

is about 90−100 °C, and depolymerization begins at 200 °C, producing a great amount of MMA. As the temperature keeps increasing, MMA will decompose to form fuel-rich substances and catch fire.[2,3,20,21] The oxygen equilibrium index of MMA was shown to be17.3.[1] This makes it easy for PMMA to sustain combustion, and then it becomes a fire hazard incipient fault. Furthermore, PMMA-exhaust emissions such as saturated and unsaturated hydrocarbons, aromatic hydrocarbons, and oxygenated organic compounds are known to be hazardous to humans, especially the numerous hydrocarbons, including 1,3-butadiene, benzene, toluene, ethylbenzene, xylene, and polycyclic aromatic hydrocarbons (PAHs); they are carcinogenic or mutagenic.[22,23] Most of the aldehydes in photochemical smog are also known to cause irritation of the skin, eyes, and nasopharyngeal membranes.[24] So more and more attention has been paid to developing the methods to promote the combustion performances and diminish the hazardous components in the exhaust, when PMMA is used as a fuel component. On the other hand, the further development of the heat resistance and the minimization of the fire hazard loss to the utmost is also inspiring. However, all these applications require a full understanding of the PMMA combustion mechanisms.

Motivated by these issues, a series of experimental investigations were performed to elucidate the thermal behaviors of PMMA, mainly focused on the thermal stability, the anaerobic thermal decomposition,[25−27] and the surface combustion of PMMA sheets, consisting of temperature field distribution and regression rate.[28−32] However, due to the lack of established on-line sensitive and selective gas monitoring techniques for the volatile organic compounds exhausted during the combustion, little research has been carried out to indentify the detailed combustion process of MMA. The structures of the combustion products could not be clearly confirmed. A lot of things stayed in mist, not only the identifications of the free radicals and the intermediates, but also the production and the destruction of these substances, not to mention the combustion mechanism in detail.

Generally, lean burning of fuels yields exceptionally low pollutant emission and superior combustion characteristics. However, the high lean flammability limit of most fuels makes it extremely difficult to achieve a stable combustion condition. Due to this extremely low limit, lean burning of fuels is quite attractive.[33]

In this work, we studied the lean premixed laminar MMA/O_2 flame by using the synchrotron VUV photoionization and molecular-beam mass spectrometry (MBMS) techniques. These techniques can detect several components simultaneously, and the high resolution of photoionization mass spectrometry (PIMS) and the tunable photon energy from synchrotron allow isomer-specific detections of the intermediates; molecular-beam sampling could cool the species efficiently. About 43 compounds formed in the MMA flame were detected by photoionization mass spectra and identified by photoionization efficiency (PIE) spectra measurements.

Experimental Methods

The sample used in this experiment was used as received: MMA (Shanghai Chemical Reagent Inc. of Medicine Group of China; purity, 99.99%; molecular weight (MWw), 100.11 g·mol^{-1}; boiling point, 100.3 °C; freezing point, −48 °C; density at 25 °C, 0.940 g·cm^{-3}; viscosity at 20 °C, 0.58 MPa·s). Experiments were performed at the flame endstation of National Synchrotron Radiation Laboratory (NSRL), Hefei, China. The synchrotron radiation from 800 MeV electron storage ring is monochromized by using a 1 m Seya-Namioka monochromator equipped with two gratings (2400 and 1200 grooves/mm) covering the wavelength range from 40 to 200 nm. The average photon flux was measured to be 5×10^{10} photons/s. MgF_2 and LiF windows (thickness = 1 mm) were used to eliminate higher-order radiation, respectively. The wavelength calibrated with the known ionization energies (IEs) of the inert gases. The energy resolution ($E/\Delta E$) is about 500−1000 depending on the width of the slits.

The experimental arrangement and procedures used for VUV photoionization sampling of the low-pressure premixed flames were reported previously.[34,35] Briefly, for investigating combustion of MMA, it mainly consists of a flat burner situated in the flame chamber, a differentially pumped flame-sampling system, and photoionization chamber with RTOFMS for photoions detection. The photoions are collected and analyzed by a reflectron time-of-flight mass spectrometer (RTOFMS) with the mass resolving power ($m/\Delta m$) of ∼1400. Ar is used as carrier gas whose flow rate is accurately controlled by a mass flow controller (MKS, USA). Low-pressure laminar premixed flame on a 6.0 cm diameter flat burner (McKenna, USA) is sampled through a quartz nozzle with an orifice diameter of ∼0.5 mm. The sampled gases pass through a nickel skimmer into a differentially pumped ionization region where it is crossed by the tunable vacuum ultraviolet (VUV) light and horizontally goes through the gap between the repeller and extractor plates of RTOFMS. Photoions are extracted using a pulsed field. Pulse voltage of the repeller plate is used to propel ions up to a multichannel plate (MCP) detector. A silicon photodiode (SXUV-100) is used to record the VUV photon intensities.

The MMA/O_2/Ar flame ($\phi = 0.75$) at a pressure of 2.67 kPa (20 Torr) was used for this study. The flow rates for O_2 and Ar were 0.845 and 0.950 SLM, respectively. The liquid flow rate of MMA, controlled by a syringe pump, was 050 mL·min^{-1} at room temperature. (For MMA, the liquid flow rate of 0.50 mL·min^{-1} is equivalent to 0.105 SLM.). The flux-normalized ion signals, measured as a function of the photon energy, yielded the PIE spectra. For PIE measurements, the quartz nozzle was located at the distance of 5.0 mm from the burner surface. The light wavelengths were altered from 115 to 160 nm, plus 0.3 nm for each measurement. The experimental error for determining IE should be within ±0.05 eV as the cooling effect of molecular beam was considered. The pressures were 1.6×10^{-4} and 1.8×10^{-5} Pa for the differential and photoionization chambers respectively. In order to obtain the accurate mole fractions of most species, fragmentation should be avoided to maintain near-threshold ionization. Therefore, we scanned the burner at selected photon energies of 16.53, 11.70, 10.78, 10.00, and 9.54 eV. The mole fractions of the species were then derived by the method described by Cool et al.[36] In the experiment, the sampling cone drew from a flame zone might extend about several nozzle diameters ahead of the cone.[37,38]

Results and Discussions

1. Identification of Flame Intermediates and Products. A photoionization mass spectrum of the MMA flame at the photon energy of 10.78 eV is shown in Figure 1. A series of peaks are detected in the spectra (Figure 1), which indicate that a lot of substances can be formed in the premixed MMA/O_2/Ar flame. The species of radicals produced in the lean flame should be less than those in the rich flame owing to excess oxygen. Relative intensities of the peaks changes as sampling positions and photon energies alter. Each mass peak can possibly be corresponded to many substances, and the total number of

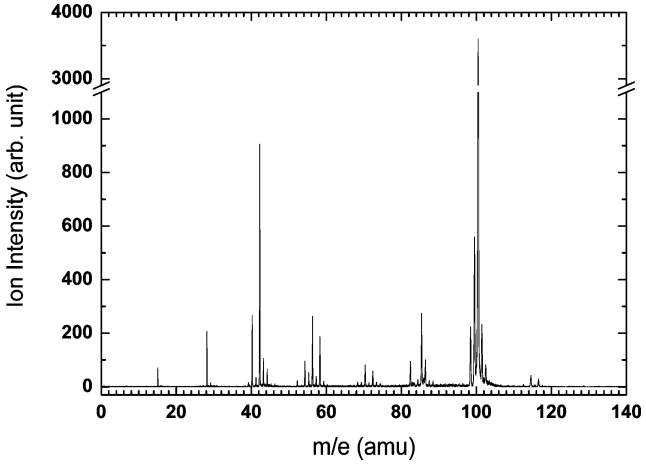

Figure 1. Photoionization mass spectrum of laminar lean premixed $MMA/O_2/Ar$ flame at the pressure of 2.67 kPa (20.0 Torr) and the photon energy of 10.78 eV, taken at the nozzle sampling position of 5.0 mm from the burner surface.

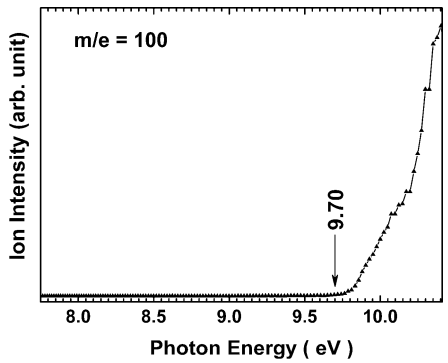

Figure 2. PIE spectra of $m/e = 100$ ($C_5H_8O_2$) measured at the nozzle sampling position of 5.0 mm from the burner surface for lean premixed $MMA/O_2/Ar$ flame.

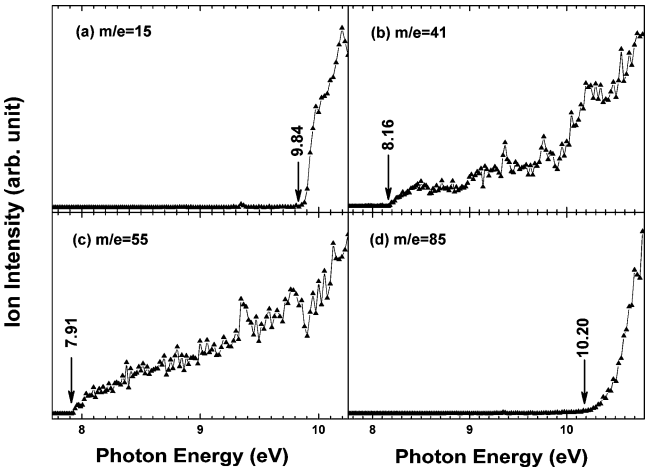

Figure 3. PIE spectra of (a) $m/e = 15$ (CH_3), (b) $m/e = 41$ (C_3H_5), (c) $m/e = 55$ (C_4H_7), and (d) $m/e = 85$ ($C_4H_5O_2$), measured at the nozzle sampling position of 5.0 mm from the burner surface for lean premixed $MMA/O_2/Ar$ flame.

possible isomers increases rapidly with the increasing of molecular weight. Therefore, identifying isomers responsible for each observed mass peak is an important step to the prediction of the combustion mechanism of MMA. To obtain PIE spectra, a series of mass spectra at a fixed burner position (5.0 mm) were recorded by scanning photon energy, and each mass peak was integrated with the background subtraction and plotted versus photon energy. Ionization energy (IE) of species can be directly obtained from the PIE spectra.[35,39−41] In this article, we display a part of the measured PIE spectra in order to identify the isomers. Some substances whose ionization energies are higher than 10.78 eV or lower than 7.75 eV, such as H_2O, CO_2, CO, etc., have not be detected in this PIE experiment and would be discussed in the mole fractions investigation. The analysis showed that there were not only monomolecular intermediates, but also free radicals in the flame. The heaviest mass detected is 116, and there was no species with *m*/*e* value around or more than 200, which indicated that MMA did not polymerize under the current experimental conditions. Furthermore, no PAHs were detected, and it could be concluded that the combustion reaction of MMA proceeded rather sufficiently due to the fuel-lean experimental condition. The high concentration of MMA detected in the flame shows that the combustion was not efficient enough at the position of 5.0 mm from the burner. The species are identified and listed in Table 1 with the measured IEs and the literature's values.

The ionization energies of species (2), (9), (10), (17), (26), (34), (36), and (39) have not been given by literature,[42] and the most probable structures are proposed based on the structure of MMA. Previous researches suggested that there was also thermal oxidative decomposition in the combustion of PMMA when oxygen existed, and resulted in MMA reacting to form some peroxides, marked as RO_2, which are unstable and break down rapidly to generate more free radicals.[43] However, no such substances were detected in this work. It was mainly because that most oxygenic free radicals were very active and easy to quench in the sampling process.

a. Methylmethacrylate (MMA). The species with the *m*/*e* value of 100 was detected, and has relatively high ion intensity as shown in Figure 1. It indicates that there is a great amount of MMA at the sampling position in the flame. The PIE spectra of this substance is shown in Figure 2, in which a sharp onset is observed at 9.74 ± 0.05 eV, and this value is in good agreement with the IE of methylmethacrylate measured by photoelectron spectroscopy. Thus, $m/e = 100$ can be attributed to methylmethacrylate radical according to the PIE measurement.

b. Free Radicals. Several kinds of radicals were detected and identified in MMA flame for the first time. The following figures are chosen to show PIE spectra for some radicals. Figure 3a shows the PIE spectra of $m/e = 15$, and there is a sharp onset observed at 9.84 ± 0.05 eV, which is in good agreement with the IE of the methyl radical measured by photoelectron spectroscopy. Thus, it can be concluded that the $m/e = 15$ is the methyl radical. Methyl is discovered to be the most abundant hydrocarbon radical in the hydrocarbon flame, and it has been reported to contribute to polycyclic aromatic hydrocarbons (PAHs) formation.[44] The PIE curve of $m/e = 41$ is presented in Figure 3b, and a clear onset is observed at 8.16 ± 0.05 eV. This value is in excellent agreement with the IE the allyl radical (8.153 eV), which was determined by zero kinetic energy photoelectron spectrometry.[45] The C_3H_5 radical is also a key intermediate in tropospheric chemistry, and is believed to play important roles in formation of PAHs, and soot in combustion processes.[46] An onset is observed from the PIE spectra of $m/e = 55$ shown in Figure 3c, which is attributed to the IE of 2-methylallyl radical according to the IE (7.90 ± 0.02 eV) given in the literature.[42] Figure 3d shows the PIE spectra of $m/e = 85$, and a clear onset is observed at 10.20 ± 0.05 eV. As there has no correlative research related to the ionization energy of this radical previously, we predicted it might be methacrylic acid radical ($C_4H_5O_2$) based on the structure of MMA. Besides

TABLE 1: Species Measured in the MMA Flame along with Their IEs, Maximum Mole Fractions (X_{max}), and Positions

				IEs (eV)		concentration	
products	mass	formula	species	this work[a]	literature[b]	position (mm)	X_{max}
(1)	15	CH_3	methyl radical	9.84	9.84 ± 0.01	6.0	4.15×10^{-3}
(2)	26	C_2H_2	CH_2C	8.59		8.0	4.19×10^{-6}
(3)	28	C_2H_4	ethylene	10.52	10.51	6.0	1.04×10^{-3}
(4)	29	C_2H_5	ethyl radical	8.47	8.51 ± 0.01	3.5	3.52×10^{-4}
(5)	39	C_3H_3	propargyl radical	8.68	8.67 ± 0.02	6.0	9.22×10^{-3}
(6)	40	C_3H_4	allene	9.70	9.69	6.0	5.04×10^{-3}
(7)	41	C_3H_5	allyl radical	8.16	8.15	6.0	6.93×10^{-4}
(8)	42	C_2H_2O	ketene	9.63	9.62	5.5	1.38×10^{-2}
(9)	43	C_2H_3O	CH_2CHO	9.88		5.0	6.64×10^{-3}
(10)	43	C_2H_3O	oxiranyl radical	9.88			
(11)	44	C_2H_4O	ethenol	9.31	9.33 ± 0.01	4.0	7.65×10^{-4}
(12)	44	C_2H_4O	acetaldehyde	10.20	10.22	5.0	1.34×10^{-3}
(13)	52	C_4H_4	1-buten-3-yne	9.60	9.58	6.0	1.12×10^{-3}
(14)	54	C_3H_2O	propadienal	9.11	9.12 ± 0.05	5.5	1.72×10^{-4}
(15)	55	C_4H_7	2-methylallyl radical	7.91	7.90 ± 0.02	5.5	6.78×10^{-4}
(16)	56	C_3H_4O	cyclopropanone	9.02	9.1 ± 0.1	5.5	4.57×10^{-3}
(17)	57	C_3H_5O	CH_2COCH_3	9.18		3.5	3.81×10^{-4}
(18)	58	C_3H_6O	methoxy-ethene	8.94	8.95 ± 0.01	4.0	5.44×10^{-3}
(19)	58	C_3H_6O	2-propen-1-ol	9.70	9.67 ± 0.03	4.5	8.85×10^{-3}
(20)	58	C_3H_6O	acetone	9.70	9.70		
(21)	59	C_3H_7O	1-methyl ethoxy radical	9.21	9.20 ± 0.05	3.0	6.72×10^{-5}
(22)	59	C_3H_7O	n-propoxy radical	9.21	9.20 ± 0.05		
(23)	68	C_4H_4O	1-buten-3-yn-2-ol	8.93	8.92	5.0	3.40×10^{-4}
(24)	69	C_5H_9	3-butenyl, 2-methyl	8.02	8.00	2.5	4.54×10^{-5}
(25)	70	C_4H_6O	(*Z*)-1,3-butadienol	8.47	8.47 ± 0.03	5.5	1.39×10^{-2}
(26)	71	C_4H_7O	$CH_3CHCOCH_3$	8.87		6.0	2.45×10^{-4}
(27)	72	C_4H_8O	tetrahydro-furan	9.40	9.40 ± 0.02	3.5	3.04×10^{-4}
(28)	72	C_5H_{12}	pentane	10.27	10.28 ± 0.10	1.0	2.17×10^{-2}
(29)	72	C_5H_{12}	2-methyl-butane	10.27	10.32 ± 0.05		
(30)	73	C_4H_9O	n-butoxy radical	9.19	9.22 ± 0.05	4.0	2.65×10^{-4}
(31)	74	$C_4H_{10}O$	methyl propyl ether	9.46	9.41 ± 0.07	2.5	1.56×10^{-4}
(32)	82	C_5H_6O	pent-1-yn-3-one	10.08	10.08	1.0	4.94×10^{-3}
(33)	84	C_6H_{12}	(*E*)-2-hexene	8.86	8.88 ± 0.02	5.0	5.15×10^{-4}
(34)	85	$C_4H_5O_2$	methacrylic acid radical	10.23		1.0	2.68×10^{-2}
(35)	86	$C_4H_6O_2$	isocrotonic acid	10.06	10.08	6.0	1.18×10^{-3}
(36)	87	$C_4H_7O_2$	1,4-dioxyl radical	9.74		3.0	7.19×10^{-5}
(37)	88	$C_4H_8O_2$	1,2-dioxane	9.96	10.0	3.5	7.37×10^{-5}
(38)	98	$C_5H_6O_2$	buta-2,3-dienoic acid, methyl ester	10.06	10.02	5.5	1.13×10^{-3}
(39)	99	$C_5H_7O_2$	methl methacrylate radical	10.10		1.0	1.47×10^{-2}
(40)	100	$C_5H_8O_2$	methylmethacrylate	9.70	9.70	0.0	5.5×10^{-2}
(41)	102	$C_5H_{10}O_2$	1,3-dioxepane	9.49	9.45	6.0	7.58×10^{-5}
(42)	114	$C_7H_{14}O$	2-ethyl-3-methyl-butanal	9.45	9.44	4.5	4.58×10^{-5}
(43)	116	$C_7H_{16}O$	2-heptanol	9.74	9.70 ± 0.03	4.5	2.17×10^{-5}

[a] Experimental error for IEs is ±0.05 eV. [b] Refers to ref 42.

the radicals discussed above, C_2H_5, C_3H_3, C_3H_5, C_2H_3O, C_4H_7, C_3H_5O, C_3H_7O, and $C_5H_6O_2$ were also detected in this work, as listed in Table 1. C_2H_5 is one of the important intermediates in combustion reaction mechanism and is a reliable indicator of flame zones, flow structure, and temperature. The C_3H_3 radical is discovered to exist in hydrocarbon flame widely, and acts as an important role in chemical-vapor deposition, and interstellar media. Also, it is considered as a precursor in the formation of benzene, PAHs, and soot in flame.[47]

c. Monomolecular Species. In the MMA flame, other molecules were also identified, including hydrocarbons and oxygenated compounds. Some species are newly detected in MMA flame, i.e., 1-buten-3-yne ($m/e = 52$), propadienal ($m/e = 54$), cyclopropanone ($m/e = 56$), methoxy-ethene ($m/e = 58$), 1-buten-3-yn-2-ol ($m/e = 68$), pent-1-yn-3-one ($m/e = 82$), and 1,3-dioxepane ($m/e = 102$). Some of the hydrocarbons are the precursors of PAHs, such as C_3H_4 and C_4H_4. Oxygenated compounds are important intermediates in the oxidation of hydrocarbons and are formed easily in the lean flame as the oxidizer is excessive. The detected oxygenated compounds are alcohols (ethenol, 2-propen-1-ol, etc.), carbonyl (acetaldehyde), ketone (cyclopropanone, acetone, etc.), ether (methoxy-ethene, tetrahydro-furan, etc.), and organic acids. Some of the compounds were found in gas products of PMMA pyrolysis and combustion of PMMA-based propellants. Figure 4 shows the PIE spectra of some molecules. The PIE spectra of $m/e = 42$ is shown in Figure 4a, and there is a sharp onset at 9.68 ± 0.05 eV, which is attributed to the IE of propene measured by photoelectron spectroscopy. Two clear onsets are observed for the PIE spectra of $m/e = 58$, as presented in Figure 4b. It corresponds to the IEs of methoxy-ethene (IE = 8.94 eV), 2-propen-1-ol (IE = 9.67 ± 0.03 eV), or/and acetone (IE = 9.70 eV), respectively. This implies that the mass 58 contains the contributions of methoxy-ethene, 2-propen-1-ol, or/and acetone. The ionization energies of 2-propen-1-ol and acetone are too similar to be distinguished in the experiments. Figure 4c presents the PIE spectra of $m/e = 70$, a clear onset can be observed at 8.47 ± 0.05 eV, which corresponds to (*Z*)-1, 3-Butadienol according to previous research using electron impact techniques. Figure 4d shows the PIE spectra of $m/e = 82$, and the IE is 10.08 ± 0.05 eV that is confirmed to be pent-1-yn-3-one. Compared to other PIE spectra, the onset for the PIE spectra of $m/e = 82$ is less obvious, and the ion intensity increases slowly as the photon energy is higher than the threshold in a certain range, which is about 0.15 eV. This phenomenon indicates that the electronic state structure of this

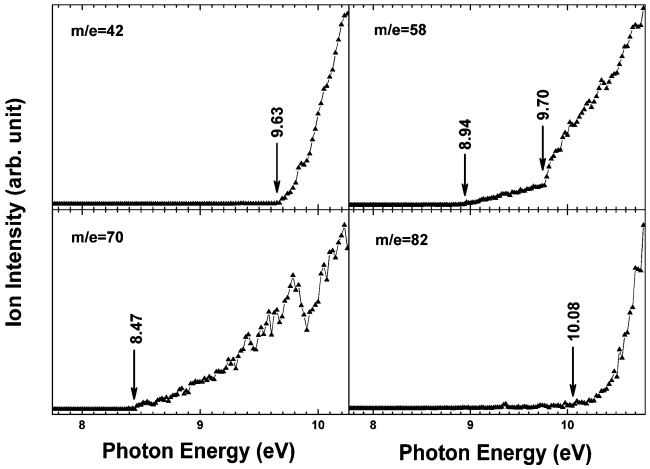

Figure 4. PIE spectra of (a) $m/e = 42$ (C_2H_2O), (b) $m/e = 58$ (C_3H_6O), (c) $m/e = 70$ (C_4H_6O), and (d) $m/e = 82$ (C_5H_6O) measured at the nozzle sampling position of 5.0 mm from the burner surface for lean premixed MMA/O_2/Ar flame.

cation is different from that of the ground state molecule. Considering Frank-Condon principle, it means that the upper electronic state structure of pent-1-yn-3-one is not the balanced structure in the relevant transition area. As the photon energy increases, the intramolecular energy distribution changes, which cause the electronic state structure transform to the equilibrium structure, and exhibits the delayed rapid increase in the PIE spectra. Moreover, some kinds of enols were also detected in the flame. Taatjes et al. first detected enols in 24 different flames of 14 prototypical single fuels by using the tunable synchrotron photoionization technique and proved that enols were common intermediates in hydrocarbon flames.[48] In this experiment, both ethanol and (*Z*)-1,3-butadienol were identified, and it would help to understand the hydrocarbon oxidation mechanism.

2. Mole Fraction Profiles. The measurement of mole fractions is very important for modeling the combustion kinetics and industrial computations. In this work, mole fractions were measured by moving the burner toward or away from the quartz nozzle at selective photon energies near ionization threshold. The mole fractions of all observed species were calculated and also listed in Table 1 along with the maximum mole fractions and their positions from the burner surface. The mole fractions have an uncertainty of ±25% for the stable intermediates and a factor of 2 for radicals. At the photon energy of 16.53 eV, as the filter range limitation of MgF_2 and LiF windows, the influence of higher-order radiation is becoming obvious, and some species are formed directly by photodissociation of some free radicals and molecules in the photoionization chamber. So these species are not involved in the discussion for combustion mechanism, i.e., $m/e = 12$, 16, 17, and 45. The substance with $m/e = 36$ is clearly observed. By comparing its ion intensity to that of Ar, it can be concluded that it is one isotope of argon. So when to calculate the mole fraction of Ar, this isotope must be considered.

a. Mole Fraction Profiles for Major Species. Mole fraction profiles for the major species including Ar, H_2O, CO, O_2, CO_2, H_2, and $C_5H_8O_2$ are displayed in Figure 5. It is obvious that all mole fraction profiles are functions of distance from the burner surface. The mole fraction of Ar decreases from 0.500 in the entering cold flow to 0.444 in the post-flame, and the concentration of H_2O and CO_2 increases along with the decrease of that of O_2. The integrated ion count for $m/e = 101$ is just about 1% of that for $m/e = 100$, so it can be concluded that $m/e = 101$ has the chemical formula of $^{13}C^{12}C_4H_8O_2$. Therefore, the mole

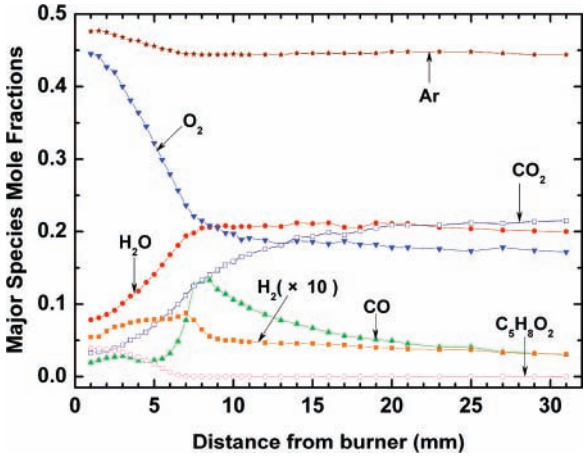

Figure 5. Mole fractions profiles for the major species: Ar, $C_5H_8O_2$, O_2, CO, CO_2, H_2O, and H_2.

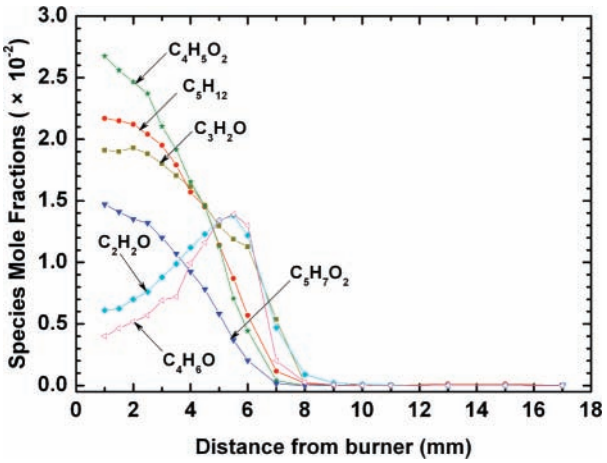

Figure 6. Mole fractions profiles for species: C_2H_2O, C_3H_2O, C_5H_{12}, C_4H_6O, $C_4H_5O_2$, and $C_5H_7O_2$.

fraction of MMA should be calculated by adding the mole fractions of $m/e = 100$ and 101 together. A very low concentration of H_2 is confirmed to be formed just above the burner surface and persist into the post-flame zone, though the amount of O_2 is excessive. It is widely known that H atom is produced with relative high abundance in both pyrolysis and combustion processes of polymers and play a very important role in the reaction system. In the near burner surface zone, it is noted that the mole fraction of CO increases with increasing the distance from the burner, reaches the highest abundance at 8.5 mm with the mole fraction of 0.133, and then decreases to 0.0299 in the post-flame. In addition, the mole fractions of CO_2, CO, H_2O, and O_2 are 0.0713, 0.0227, 0.141, and 0.322 when the sampling position is located at 5.0 mm from the burner surface. The CO_2/CO ratio is equal to 3.14, less than 10, and the mole fraction of oxygen is more than 0.15. Therefore, we could classify this MMA fire to be a kind of fully developed (flaming) fire,[49] which means it has a relative low CO levels toxicity, and the rate of fuel consumption continues to increase until it is limited by the availability of oxygen. The mole fractions of H and O radicals are not provided because of their high chemical activity and could not be cooled effectively by molecular beam sampling.

b. Mole Fraction Profiles for Other Flame Species. The mole fraction profiles for other 36 flame species are displayed in Figures 6−11. These profiles are presented in order of abundances from highest in Figure 6 to lowest in Figure 11. Regions of more intense chemical activity are found to be between 1 mm to 10 mm above the burner surface. Radicals are key

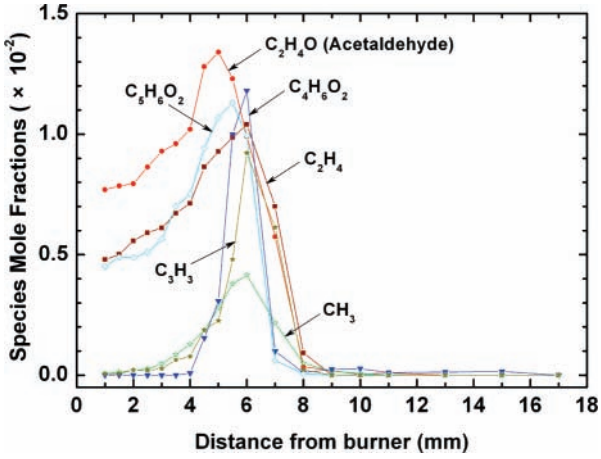

Figure 7. Mole fractions profiles for species: CH_3, C_2H_4, C_3H_3, C_2H_4O (acetaldehyde), $C_4H_6O_2$, and $C_5H_6O_2$.

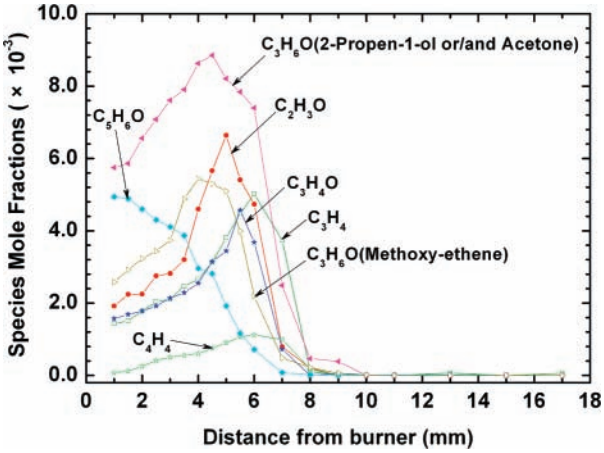

Figure 8. Mole fractions profiles for species: C_3H_4, C_2H_3O, C_4H_4, C_3H_4O, C_3H_6O (methoxyethane), $C_3H_6O_2$ (2-propen-1-ol or/and acetone), and C_5H_6O.

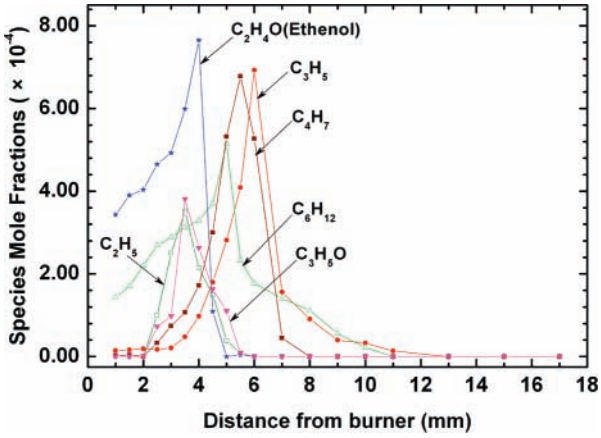

Figure 9. Mole fractions profiles for species: C_2H_5, C_3H_5, C_4H_7, C_2H_4O (ethenol), C_3H_5O, and C_6H_{12}.

intermediates in combustion chemistry. To obtain their concentration at different stages of combustion is essential for accurate prediction of the flame behaviors and properties. But compared with the concentration measurement of stable species, the concentrations of radical are more difficult to measure.[50] In this work, the mole fractions of most detected free radicals, including C_2H_5, C_3H_3, C_3H_5, C_4H_7, etc., were calculated, and the maximum mole fractions of most free radicals are around $\sim 10^{-4}$. It is noted that some of the species have the highest abundances around the same position near the burner surface,

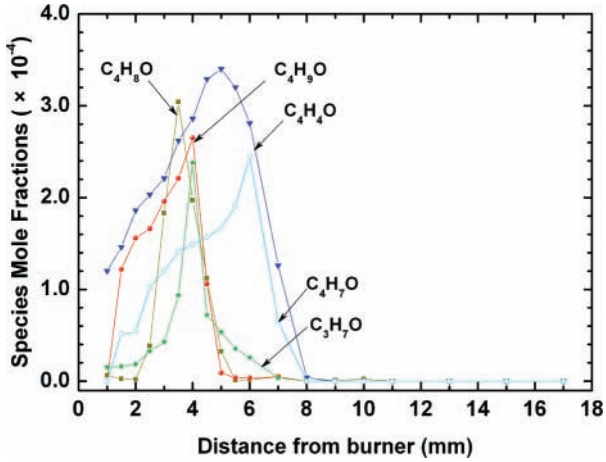

Figure 10. Mole fractions profiles for species: C_3H_7O, C_4H_4O, C_4H_7O, C_4H_8O, and C_4H_9O.

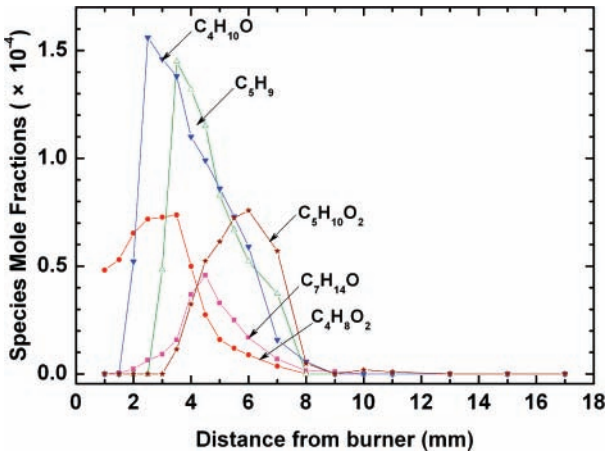

Figure 11. Mole fractions profiles for species: C_4H_{10}, C_5H_9, $C_4H_8O_2$, $C_7H_{14}O$, and $C_5H_{10}O_2$.

and then decrease, such as $C_4H_5O_2$, $C_5H_7O_2$, C_5H_6O, and C_5H_{12}. These species are easily formed in the low-temperature reaction zone, act as the precursors, or take part in the formation of most other detected species, whose abundances reach the peak value at some distances far from the burner, such as C_3H_4O, C_3H_6O, $C_4H_6O_2$, and $C_7H_{14}O$.

3. Combustion Mechanism of Fuel-Lean Premixed MMA/O_2/Ar. According to the identification of the species in the MMA flame, it can be inferred that pyrolysis of MMA and O_2 takes place at the initial reaction stage, form some radicals and intermediates, such as (1) methyl radical, (2) CH_2C, (34) methacrylic acid radical, and (39) methyl methacrylate radical. Considered the mole fraction profiles and the relationship among the relevant species, we could further study the combustion mechanism. The pyrolysis is discussed in the following reactions, in which the substances numbers are consistent with the consecutive Arabic numbers in Table 1.

a. Pyrolysis of MMA and O_2.

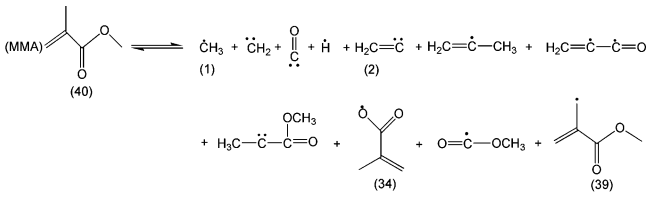

$O_2 \rightleftharpoons 2\,\dot{O}$

b. Free Radical Reaction. The free radicals produced during the pyrolysis may act as precursors of many detected species. Some of the radicals formed the unimolecules by internal lone pair electrons of free radicals self-bonding directly, such as ·C═O and H_2C═C·—C·═O, others formed the final products or intermediates by self-addition reaction or reacting with other free radicals, such as (13), (18), (35), and so forth. The reaction processes can be explained as follows.

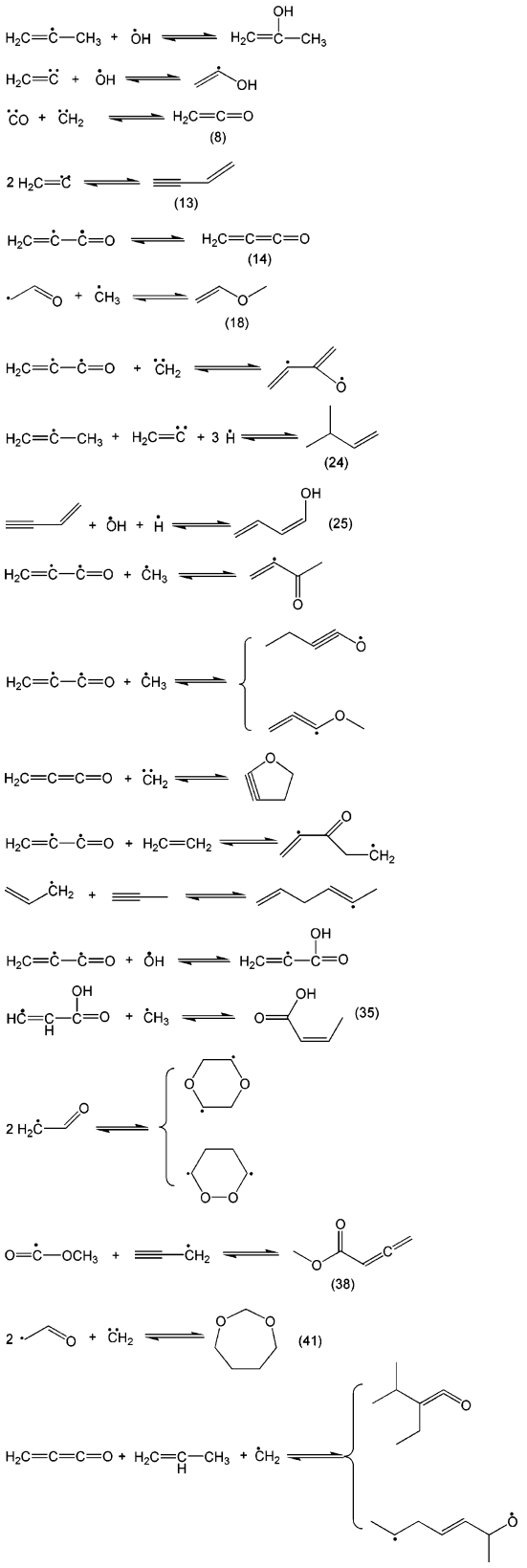

c. H-Addition Reaction. Meanwhile, some intermediates formed through reaction types *a* and *b* discussed above might add one or several hydrogen radicals to produce the species identified in the experiment. The following reactions illustrate the processes.

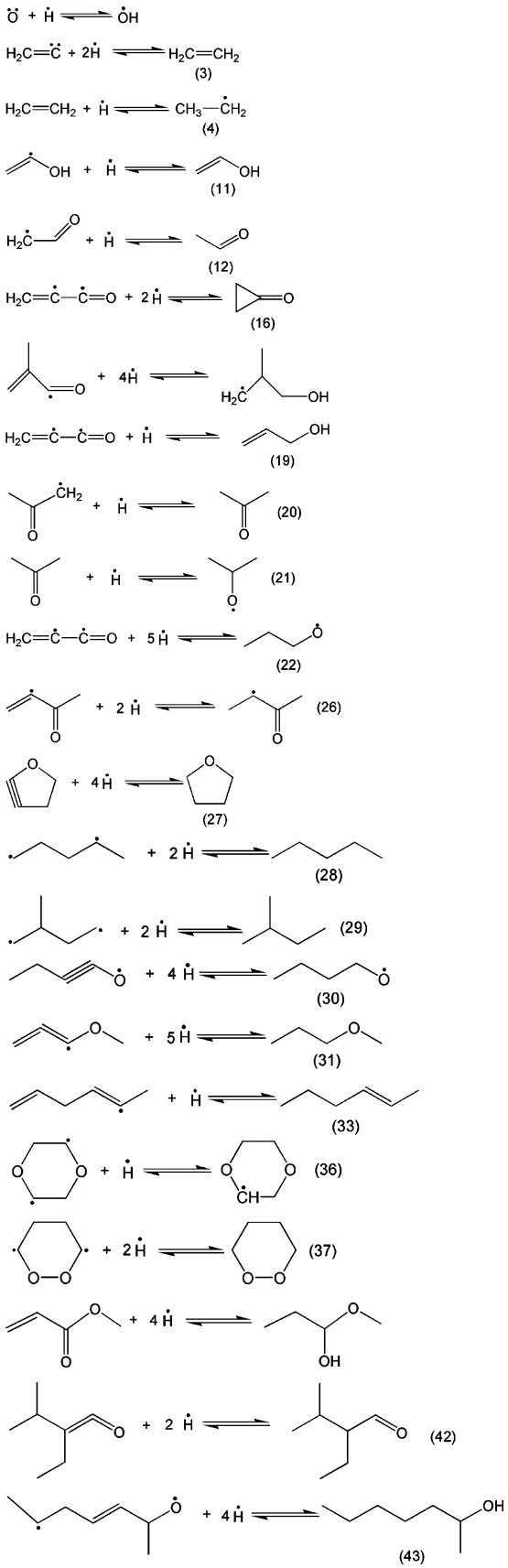

d. H-Migration Reaction. H-migration reaction means migration of a hydrogen atom and the group of atoms that are attached to it from one position in a radical into a new position, and it also plays a role in formation of some intermediates. The reaction processes can be explained as follows.

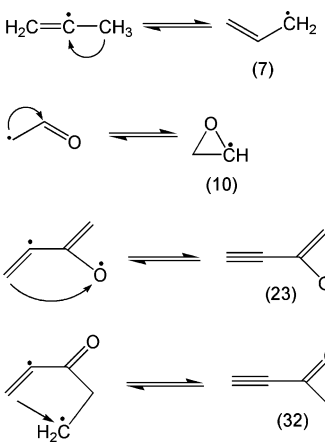

e. Dehydration Reaction. Besides the reaction types above, there is also dehydration reaction, which is usually defined as a chemical reaction that involves the loss of water from reacting molecule.

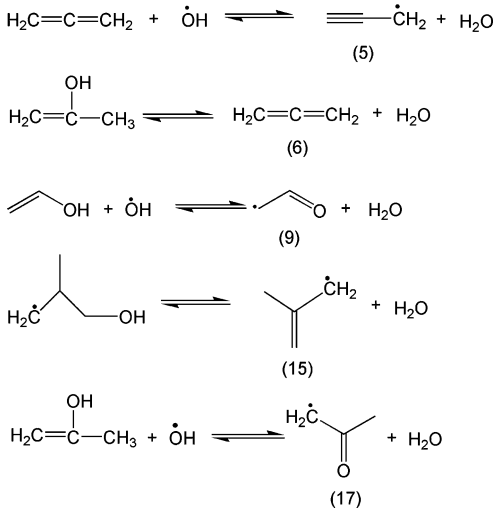

According to all of the reactions discussed in detail before, it can be concluded that the combustion of fuel-lean premixed MMA/O_2/Ar under low pressure approximates to a chain reaction system. It starts from the pyrolysis of MMA and O_2, which could be considered as the chain initiation step. In this process, a great deal of free radicals and molecules are generated, and the reactions among them sustain the chain propagation. Afterward, the chain termination took place by forming the final products, including linear termination, quadratic termination, and multiple termination. It shows that intensification of the MMA/O_2/Ar combustion is through the formation of active free radicals, such as O, OH, H, CH_3, C_3H_5, and C_3H_2O. These radicals act as important chain carriers. Especially, bi-radical C_3H_2O was discovered to be a key component and take part in the formation of many intermediates and products. The characteristic of the extra-equilibrium radical concentrations change, which is dependent on the conditions of the combustion and the distances from the burner, is determined.

Conclusions

The combustion of fuel-lean premixed MMA/O_2/Ar was studied by using the tunable synchrotron VUV photoionization and molecular-beam mass spectrometry. A lot of low molecular weight components and active radicals were detected and identified by the measurements of the photoionization mass spectrum and the PIE spectra. No PAHs were formed in the flame under the fuel-lean condition. The formation mechanisms of the species were discussed. The results showed that the combustion of MMA almost contained two processes, which were the pyrolysis of MMA and O_2, and the chain reactions of free radicals and intermediates, respectively. C_3H_2O was found to be the key radical in the whole combustion process for the first time. Intensification of the combustion due to an increase in reaction activity resulting from MMA thermal decomposition was demonstrated. Based on the composition data, the mole fractions of the flame species were measured by scanning the burner near the ionization threshold at selective photon energies.

Acknowledgment. The authors thank National Synchrotron Radiation Laboratory for providing beamtime for performing the experiments. This work is supported by the National Nature Science Foundation of China (No. 50476025).

References and Notes

(1) Fenimore, C. P.; Martin, F. J. *Combust. Flame* **1966**, *10*, 135−139.
(2) Van Der Geld, C. W. M.; Korting, P. A. O. G.; Wijchers, T. *Combust. Flame* **1990**, *79*, 299−306.
(3) Harper, C. A. *Modern Plastics Handbook*; Mcgraw-Hill Companies, Inc.: New York, 2000.
(4) Brokenbrow, B. E.; Sims, D.; Stokoe, A. L. *UK Defense Technical Report AD0880956*.
(5) Ishiharaa, A.; Sakaia, Y.; Konishia, K.; Andoh, E. *Proc. Combust. Inst.* **2005**, *30*, 2123−2130.
(6) Karabeyoglu, M. A.; Zilliac, G. *AIAA* 2003, 1162.
(7) Kappenstein, C.; Batonneau,Y. *AIAA* 2005, 3920.
(8) Matticari, G.; Noci, G. E.; Siciliano, P. *AIAA* 2006, 4872.
(9) Micci, M. M.; Ketsdever, A. D. *Micropropulsion for Small Spacecraft*; AIAA: Reston, VA, 2000; p 45.
(10) Haag, G.; Sweeting, M.; Richardson, G. 13th Annual AIAA/USU Conference on Small Satellites; Logan, Utah, 1999.
(11) Nakamuraa,Y.; Kashiwagib, T.; Olsonc, S. L.; Nishizawad, K.; Fujitad, O.; Itod, K. *Proc. Combust. Inst.* **2005**, *30*, 2319−2325.
(12) Hirata, T.; Kashiwagi, T.; Brown, J. E. *Macromolecules* **1985**, *18*, 1410−1418.
(13) Seshadri, K.; Williams, F. A. *J. Polym. Sci.* **1978**, *16*, 1755−1778.
(14) Krishnamurthy, L.; Williams, F. A. *Proc. Combust. Inst.* **1972**, *14*, 1151−1164.
(15) Tsai, T. H.; Li, M. J.; Shih, I. Y.; Jih, R.; Wong, H. C. *Combust. Flame* **2001**, *124*, 466−480.
(16) Zeng, W. R.; Li, S. F.; Chou, Y. J. *Polym. Mater. Sci. Eng.* **2003**, *6*, 183−186.
(17) Di Blasi, C.; Crescitelli, S.; Russo, G.; Cinque, G. *Combust. Flame* **1991**, *83*, 333−344.
(18) Rhodes, B. T.; Quintiere, J. G. *Fire Safety J.* **1996**, *26*, 221−240.
(19) Brescianini, C. P.; Yeoh, G. H.; Chandrasekaran, V.; Yuen, R. *Combust. Sci. Technol.* **1997**, *129*, 321−345.
(20) Ito, A.; Kudo, Y.; Oyama, H. *Combust. Flame* **2005**, *142*, 428−437.
(21) Esfahani, J. A.; Kashani, A. *Heat Mass Transfer* **2006**, *42*, 569−576.
(22) Marr, L. C.; Kirchstetter, T. W.; Harley, R. A. *Environ. Sci. Technol.* **1999**, *33*, 3091−3099.
(23) Al-Farayedhi, A. A. *Int. J. Energy Res.* **2002**, *26*, 279−289.
(24) Mitchell, C. E.; Olsen, D. B. *J. Eng. Gas Turbines Power* **2000**, *122*, 603−610.
(25) Arisawa, H.; Brill, T. B. *Combust. Flame* **1997**, *109*, 415−426.
(26) Ganesh, K.; Latha, R.; Kishore, K. *J. Appl. Polym. Sci.* **1997**, *66*, 2149−2156.
(27) Montaudo, G.; Puglisl, C.; Samperi, F. J. *Polym. Sci. A.* **1998**, *36*, 1873−1874.
(28) Chaiken, R. F.; Andersen, W. H.; Barsh, M. K.; Mishuck, E.; Moe, G.; Schultz, R. D. *J. Chem. Phys.* **1960**, 32, 141−146.

(29) Blazowski, W. S.; Cole, R. B.; McAlevy, R. F., III. *Proc. Combust. Inst.* **1973**, *14*, 1177−1186.
(30) Krishnamurthy, L.; Williams, F. A. *Proc. Combust. Inst.* **1973**, *14*, 1151−1164.
(31) Hertzberg, M.; Zlochower, I. A. *Combust. Flame* **1991**, *84*, 15−37.
(32) Ishihara, A.; Sakai, Y.; Konishi, K.; Andoh, E. *Proc. Combust. Inst.* **2000**, *28*, 855−862.
(33) Choudhuria, A. R.; Gollahallib, S. R. *Int. J. Hydro. Ener.* **2004**, *29*, 1293−1302.
(34) Huang, C. Q.; Yang, B.; Yang, R.; Wang, J.; Wei, L. X.; Shan, X. B.; Sheng, L. S.; Zhang, Y. W.; Qi, F. *Rev. Sci. Instrum.* **2005**, *76*, 126108.
(35) Qi, F.; Yang, R.; Yang, B. B.; Huang, C. Q.; Wei, L. X.; Wang, J.; Sheng, L. S.; Zhang, Y. W. *Rev. Sci. Instrum.* **2006**, *77*, 084101.
(36) Cool, T. A.; Nakajima, K.; Taatjes, C. A.; McIlroy, A.; Westmoreland, P. R.; Law M. E.; Morel, A. *Proc.Combust. Inst.* **2005**, *30*, 1681−1688.
(37) Fristrom, R. M. *Flame Structure and Process*; Oxford: New York, 1995; p 175.
(38) Hartlieb, A. T.; Atakan, B.; Kohse-Höinghaus, K. *Combust. Flame* **2000**, *1214*, 610−624.
(39) Yang, B.; Osswald, P.; Li, Y. Y.; Wang, J.; Wei, L. X.; Tian, Z. Y.; Qi, F.; Kohse-Höinghaus, K. *Combust. Flame* **2007**, 148, 198−209.
(40) Cool, T. A.; Nakajima, K.; Mostefaoui, T. A.; Qi, F.; McIlroy, A.; Westmoreland, P. R.; Law, M. E.; Poisson, L. *J. Chem. Phys.* **2003**, *119*, 16, 8356−8365.
(41) Wang, T. F.; Li, S. F.; Yang, B.; Huang, C. Q.; Li, Y. Y. *J. Phys. Chem. B.* **2007**, *111*, 2449−2456.
(42) NIST website, *http://webbook.nist.gov/*.
(43) Song, J.; Fischer, C. H.; Schnabel, W. *Polym. Degrad. Stab.* **1992**, *36*, 261−266.
(44) Richter, H.; Howard, J. K. *Phys. Chem. Chem. Phys.* **2002**, *4*, 2038−2055.
(45) Gilbert, T.; Fischer, I.; Chen, P. *J. Chem. Phys.* **2000**, *113*, 561−566.
(46) Leung, K. M.; Lindstedt, R. P. *Combust. Flame* **1995**, *102*, 129−160.
(47) Miller, J. A.; Melius, C. F. *Combust. Flame* **1992**, *91*, 21−39.
(48) Taatjes, C. A.; Hansen, N.; McIlroy, A.; Miller, J. A.; Senosiain, J. P.; Klippenstein, S. J.; Qi, F.; Sheng, L. S.; Zhang, Y. W.; Cool, T. A.;Wang, J.; Westmoreland, P. R.; Law, M. E.; Kasper, T.; Kohse-Höinghaus, K. *Science* **2005**, *308*, 1887−1889.
(49) Toxicity testing of fire effluents - Part 1 Technical Report 9122−1(1989) (E). International Organization for standardization, Geneva, Switzerland.
(50) Simmie, J. M. *Prog. Energy Combust. Sci.* **2003**, *29*, 599−634.